ELSEVIER

Journal of Structural Geology 28 (2006) 1396–1405

JOURNAL OF STRUCTURAL GEOLOGY

www.elsevier.com/locate/jsg

Vein deflections and thickness variations of epithermal quartz veins as indicators of fracture coalescence

G.S. Nortje [a,b,*], J.V. Rowland [a], K.B. Spörli [a], T.G. Blenkinsop [b], S.D.C. Rabone [c]

[a] *Department of Geology, University of Auckland, Auckland, New Zealand*
[b] *School of Earth Sciences, James Cook University, Townsville, Qld. 4811, Australia*
[c] *P.O. Box 99 732 Newmarket, Auckland, New Zealand*

Received 13 January 2006; received in revised form 16 May 2006; accepted 17 May 2006
Available online 30 June 2006

Abstract

Epithermal quartz veins at the Broken Hills gold deposit, New Zealand, strike N-S and dip steeply westward. Small changes in the orientations of the three main lodes and associated mesoscopic veins define deflection lines that rake steeply in the vein plane. A method of constructing the opening vector from the three-dimensional geometry of a vein deflection is presented. The resulting vectors plunge steeply and are at low angles to the main veins and the deflection lines, indicating a large component of normal dip-slip shear during the opening of these veins. Vein thickness distributions are power-law, with similar fractal dimensions to previously reported values for non-stratabound vein arrays. The vein system at Broken Hills developed by linking of isolated extension-dominated shear veins with shear-dominated veins, generating sub-vertical and sub-horizontal fluid flow pathways.

Keywords: Opening vector; Normal dip-slip; Vein deflection; Extension veins; Extensional shears; Fault linkage; Fluid flow; Epithermal

1. Introduction

Vein opening vectors are one of the most fundamental yet elusive aspects of vein geometry. They are critical for making the important distinction between extension and extensional shear veins. Faults combined with these two types of veins form meshes which can provide fluid pathways through the rockmass, with the junctions between the structural elements controlling the directions of focussed flow and ultimately facilitating the deposition of precious metals (Cox et al., 2001; Sibson, 1987, 2001; Wilkinson and Johnston, 1996). However, piercing point analyses for opening vectors can rarely be done. There is an increasing appreciation of the limited circumstances in which fibres in veins can be directly related to opening vectors (Cox, 1987; Koehn et al., 2000; Smith, 2005; Urai et al., 1991), leaving inclusion trails as one of the most reliable methods (Cox, 1987; Koehn and Passchier, 2000; Ramsay, 1980). Many veins do not have inclusion trails, and even where they are present, inclusion trail analyses generally require considerable time and many thin sections. The problem of deducing vein opening vectors is particularly acute with respect to epithermal veins, which may occur in wide range of patterns ranging from simple veins to stockworks (Gadsby et al., 1989), and in which reliable kinematic indicators are rarely developed; moreover the materials filling veins can record post-rather than syn-opening events. This problem underlies the even greater difficulty of understanding epithermal vein mechanics, except in cases where straightforward fault/vein relationships can be directly related to stress fields (Rowland and Sibson, 2004).

An important influence on vein geometry is the history of the vein network, particularly with respect to permeability and fluid pathways (Cox et al., 1991). The measurement of

* Corresponding author. School of Earth Sciences, James Cook University, Townsville, Qld. 4811, Australia. Tel.: +61 7 4781 6397; fax: +61 7 4725 1501.
E-mail address: gustav.nortje@jcu.edu.au (G.S. Nortje).

0191-8141/$ - see front matter © 2006 Elsevier Ltd. All rights reserved.
doi:10.1016/j.jsg.2006.05.006

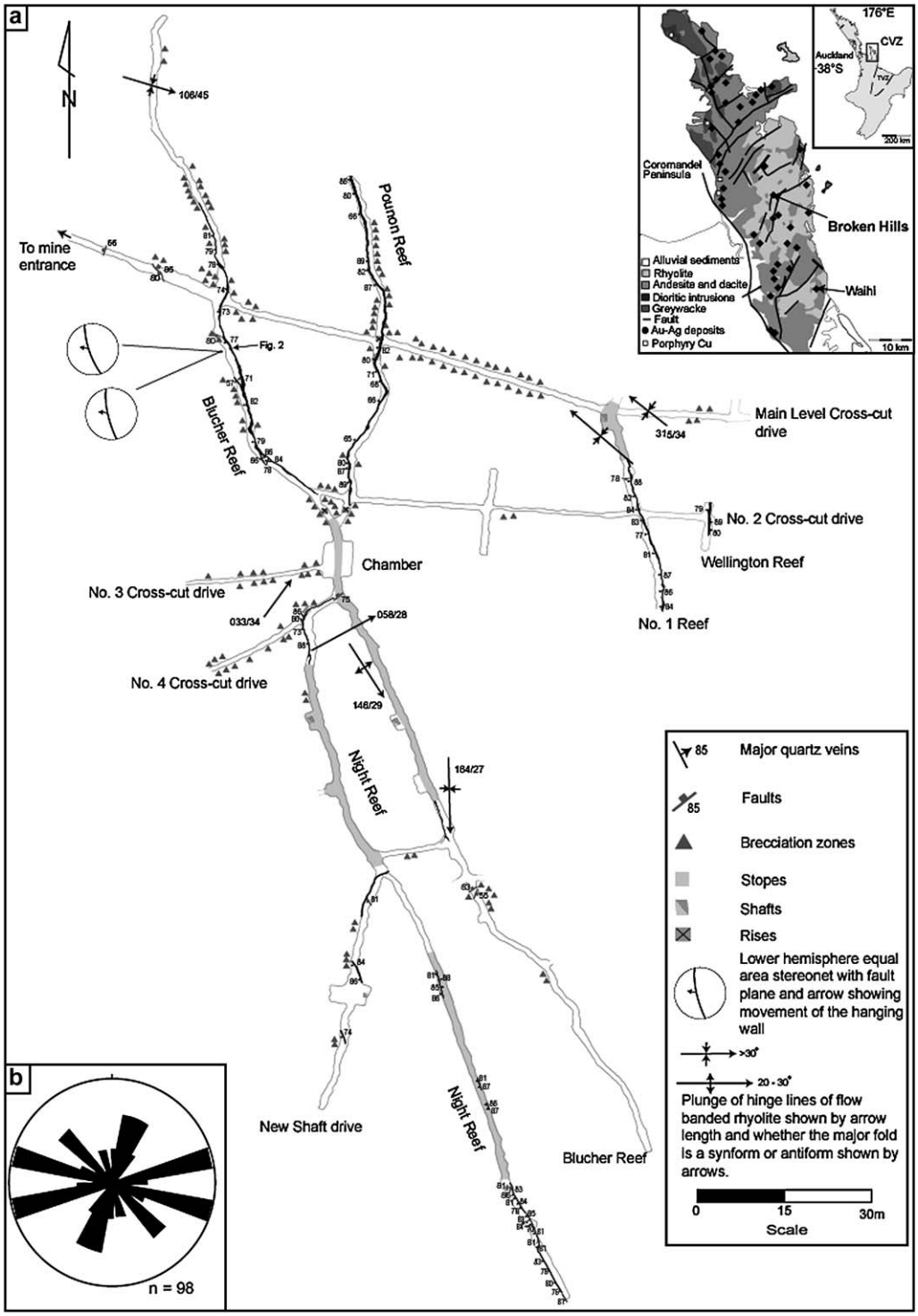

Fig. 1. (a) Simplified geological map of Broken Hills epithermal Au-Ag deposit (Nortje, 2004). All stereonets are equal area, lower hemisphere. Inset shows major geological and structural features of the Coromandel Peninsula. The locations of epithermal deposits are shown and the North Island, New Zealand with the locations of the Coromandel Volcanic Zone (CVZ) and the Taupo Volcanic Zone (TVZ) (Brathwaite and Christie, 1986; Brathwaite et al., 1989; Christie and Brathwaite, 1986; Skinner, 1986). (b) Rose diagram of breccia veins (Nortje, 2004). Rose petals contain 20 veins.

vein thickness distributions is a key method for understanding the evolution of vein networks (Johnston and McCaffrey, 1996; Lorgia, 1999; McCaffrey and Johnston, 1996; Roberts et al., 1999; Stowell et al., 1999). Vein thickness distributions in non-stratabound arrays are typically fractal (in contrast to stratabound arrays: Gillespie et al., 1999) and obey the relationship

$$N > b \sim b^{-c}, \tag{1}$$

where N = cumulative number of extension veins/shears, b = vein thickness, c = fractal dimension (cf. (Marrett, 1996)), with c varying between 0.5 and 1.5 (Gillespie et al., 1999; Sanderson et al., 1994). Gillespie et al. (1999) suggested that mineralization was restricted to non-stratabound vein arrays, and Roberts et al. (1999) have shown how c may vary through the evolution of permeability in a vein network. The fractal dimension can also be related to gold grade in mineralised veins (Sanderson et al., 1994).

The aim of this study is to present a method for evaluating vein opening kinematics which is applicable to veins with non-planar geometries, and to integrate results from this method with a study of the vein thickness distributions to gain insight into the evolution of an epithermal vein system. The study is based on the excellent three-dimensional exposures of a vein network at the Broken Hills gold deposit in the Coromandel Peninsula, New Zealand.

2. Geological framework

From 15 Ma to 6 Ma, the Coromandel Peninsula, New Zealand was the site of arc volcanism associated with a subduction system trending northwesterly and lying to the east of Coromandel Peninsula (Fig. 1a) (Ballance, 1976). Volcanic products ranged from andesitic in the older centres to rhyolitic in the younger ones. Gold mineralisation occurred in the late stages of volcanism approximately 7 to 6 million years ago (Brathwaite et al., 1989). The Hauraki Goldfield has produced 1.37 million kg of gold-silver bullion (Brathwaite et al., 1989; Christie and Brathwaite, 1986). The major producer at present is Martha Mine in Waihi (Brathwaite et al., 1989), and Fig. 1a).

2.1. Broken Hills geology

Broken Hills is hosted in 5 Ma flow-banded rhyolites that are overlain by associated pyroclastic rocks. Surface sinter remnants located to the east of the deposit indicate that the paleo-thermal watertable was at approximately 150 m a.s.l. Given that the lowest mined level is at sea-level, gold deposition at Broken Hills most likely occurred over at least the uppermost 150 m of a fossil geothermal system.

Three major veins (Fig. 1a) hosted 1700 tons of gold-silver bullion mined out from 1899–1912 (Bell and Fraser, 1912). Although generally striking north-south, these structures are characterised by abrupt changes in vein orientation and thickness at the scale of observation (Nortje, 2004). The Blucher Reef has a general NNW strike, generally dips ~75° WSW, with vein widths ranging from 10–90 cm, and mined grades of 15–20 g/t Au and 30 g/t Ag. The reef commonly exhibits banded quartz along its margins with a central zone comprising variable amounts and ratios of vein breccia, vein mixture, fine-grained hydrothermal quartz and clay gouge (Fig. 2). Vein mixture is microcrystalline brecciated vein material, most likely analogous to fault gouge.

The Pounon Reef, the second major structure along the main crosscut drive, is a splay branching north off the footwall of the Blucher Reef (Fig. 1a). It extends for ~85 m along a northerly strike and dips steeply to the west. A zone of intense brecciation occurs at the Pounon-Blucher Reef intersection. Vein thickness ranges from 10–50 cm with an average mined grade of 5 to 40 g/t Au. At its northernmost extent, the vein thins into a clay gouge-bearing shear zone.

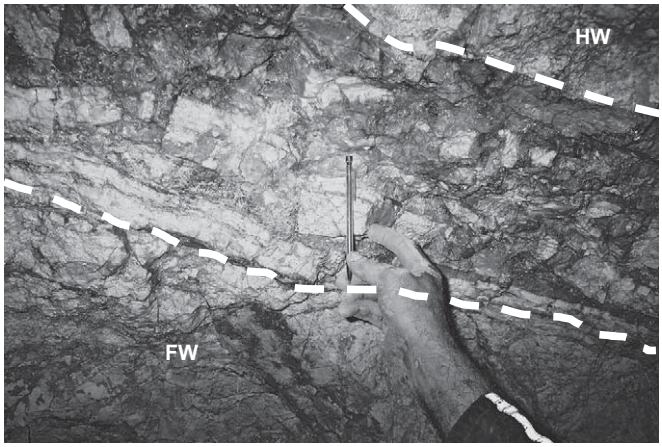

Fig. 2. Banded quartz along vein margins of the Blucher Reef (see Fig. 1a for location) with angular pieces of quartz that have been re-brecciated back into the vein. Hangingwall (HW) and footwall (FW) margins are shown by white dashed lines (Nortje, 2004).

The Night Reef was only mined in the Battery Level (Fig. 1a). Where exposed, it occurs as banded quartz veneer on footwall and hanging wall surfaces. The vein formation is about 30–90 cm wide, with a NNE strike and steep dip to the WSW. However, at its northernmost extent it bends sharply to the east to intersect the hanging wall of the Blucher Reef. In this vicinity, the vein and host rock are extensively brecciated.

The No. 1 Reef is the third major reef intersected along the main crosscut drive and has an orientation similar to the other major reefs (Fig. 1a). Its northern half is currently inaccessible because of unstable ground. Mined grades of the stopped section were approximately 15 g/t Au but unmined sections have an average grade of <3 g/t Au. The No. 1 Reef is brecciated and puggy. Vein thicknesses range from 10–30 cm.

Breccia veins are typically 1–5 cm in size, comprising brecciated host rock and quartz vein fragments. Dominant orientations for breccia veins are WSW-ENE and WNW-ESE (Fig. 1b). There is no documented evidence to suggest that these structures carry gold.

3. Vein separation, movement planes and the vector of vein opening

For vein segments of different orientation and thickness to be linked, they may have opened in the same phase of deformation. In our example this assumption is supported by the continuity of quartz vein fills through the geometric patterns at the deposit scale. In addition we make the simplifying assumption that over the lengths analysed the two walls of any vein segment are parallel.

A vein deflection is the junction between two planar, differently oriented vein segments. Depending on the angle between

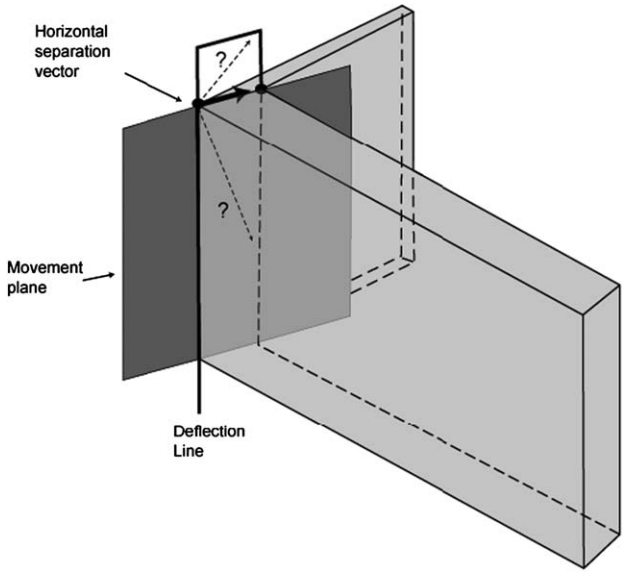

Fig. 3. Geometry of separation of linked, unequal vein segments (grey). The vector of vein opening is not defined (dotted lines with question marks) but must lie within the movement plane defined by the deflection line and the horizontal separation vector (Nortje, 2004).

them, the two segments may be of equal or unequal thickness. Where two vein segments meet (Fig. 3), there will be two parallel deflection lines (Gadsby et al., 1989). They define the movement plane, which must contain the opening vector. However with the geometry as given, the vector is not defined. Any distance measured between the two deflection lines is therefore only a separation (as used in fault analysis, (Ramsay and Huber, 1983)) and not necessarily any indication of the actual opening vector. Since the deflections lines are all steep in our example, we will use the separation in a horizontal section (= horizontal separation) to compare the geometry of various deflections (Fig. 3) because this gives an approximately cross-sectional view of the veins.

The asymmetry of the vein deflection can be described by the terms 'dextral' and 'sinistral' (Fig. 4a) in analogy to the geometry of extensional jogs (Sibson, 1996). They relate to the sense of shear implied by the vein opening if the thinner vein segment is assumed to have experienced the larger component of shear.

Where there is more than one pair and differently oriented deflection lines on vein segments that are opening simultaneously, there will be differently oriented movement planes (Fig. 4). Since each one of these is a locus of the slip vector, their statistical intersection line defines the opening vector for the system.

4. Broken Hills veins

Measurements of mesoscopic vein segments were made on Blucher Reef, Pounon Reef and No 1 (Fig. 1a). In each case, the strike and dip and the thickness of each segment was recorded. Examples where a deflection line was exposed in the outcrop were specially noted.

The steep attitudes of vein segments and their westerly dips are evident from the stereonets in Fig. 5. While N-S strikes are common, there are also NE and a few NNW trends. The thinnest vein segments appear to have a greater range in orientation but this could be due to sampling bias because more thinner veins were measured. Otherwise there appear to be no significant differences in orientation patterns related to thickness of the veins. The spread in strike is due to the presence of simple vein deflections.

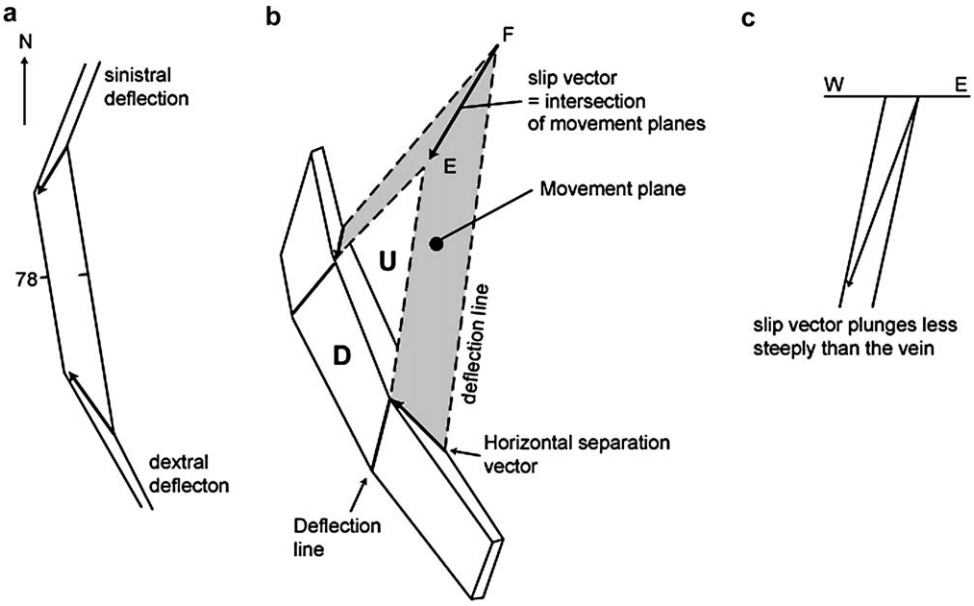

Fig. 4. Construction of the opening vector for a vein system with two sets of differently oriented deflection lines, from an actual example. (a) view of the vein system in a horizontal plane. 'Dextral' and 'sinistral' relate to the sense of rotation of the vein orientation as seen looking from the thinner to the thicker segment. (b) construction of the opening vector from the intersection of two movement planes. (c) cross-sectional view of the opening vector (Nortje, 2004).

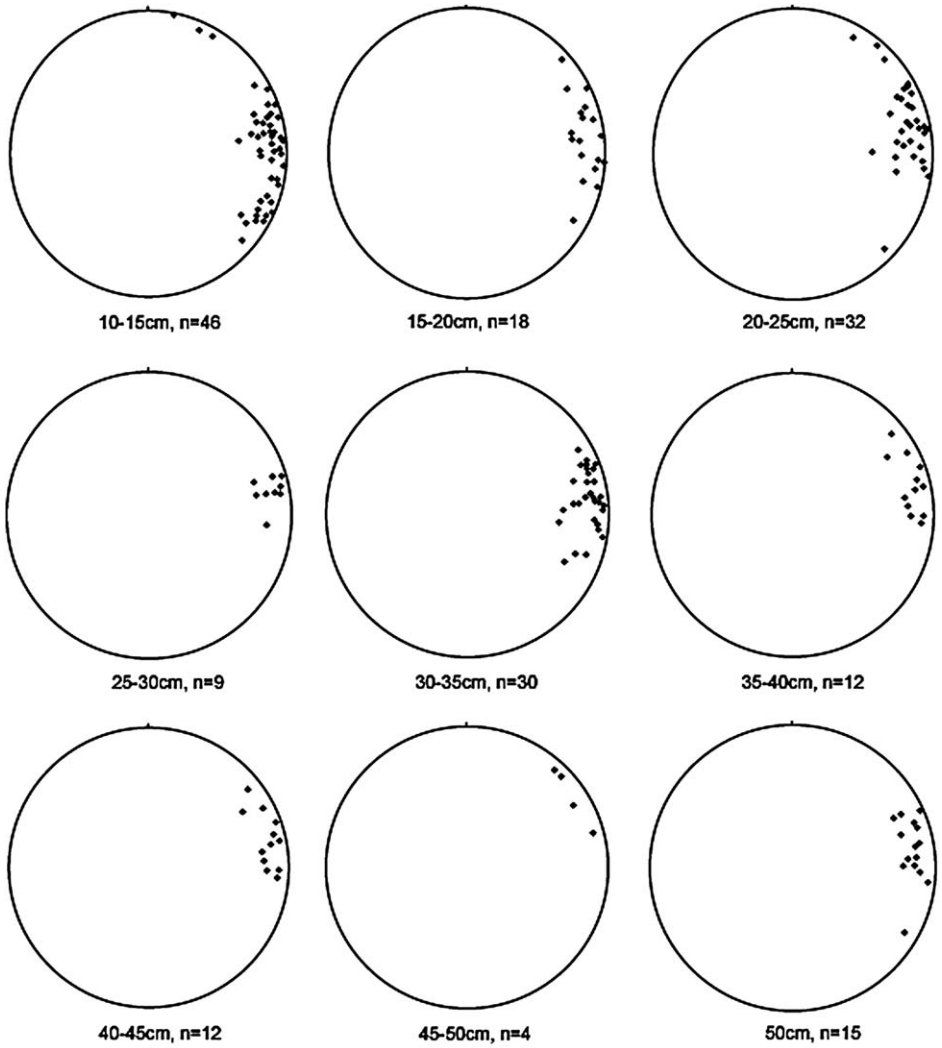

Fig. 5. Lower hemisphere equal area nets showing poles to mesoscopic veins, grouped by thickness intervals. Orientations of thinner veins appear to be more variable than those of the thicker veins. The concentration of the poles near the margins of the nets indicate that the variation in orientation is governed by a steeply west-plunging deflection axis (Nortje, 2004).

5. Thickness variations versus orientation in the mesoscopic veins

On a stereonet, the poles of the two segments in a vein deflection can be connected by a partial great circle representing a plane (Fig. 6). The pole to this plane is the deflection line. In our case these deflection lines all plunge steeply to the west. This is similar to the orientation of the deflection lines obtained from segments in the main lodes, indicating a scale invariance of these structures (Acocella et al., 2000).

The asymmetries of the vein deflections are dominantly dextral at Blucher Reef (Fig. 7a), dominantly sinistral at Pounon Reef (Fig. 7b), and bimodal at No 1 Reef (Fig. 7c).

As a further step, to visualize the vein opening in a plane at a high angle to the deflection line, we constructed horizontal sections through the vein deflections, also showing the horizontal separation vectors (Fig. 8). Especially at Pounon Reef and No. 1 Reef, the sinistral and dextral separation vectors form two distinctly oriented groups, with the lengths of the vectors showing reasonable similarity (Fig. 7). This indicates that the veins all opened in the same event. Fig. 4 shows how the difference in vector orientation is created in such a system. Note that in all three locations the dextral and sinistral separation vectors have similar general orientations.

5.1. The opening vectors

The considerations above indicate that it is possible to construct opening vectors as defined in Fig. 4 for these vein systems, by using the full three-dimensional geometry of the vein deflections. The movement planes of the deflections can be obtained by combining the separation vectors constructed in Fig. 8 with the corresponding deflection lines. In each case the statistical intersection line of all the movement planes should represent the opening vector.

The resulting opening vectors (Fig. 8) all plunge steeply west and are at a low angle to the vein dip and to the vein walls

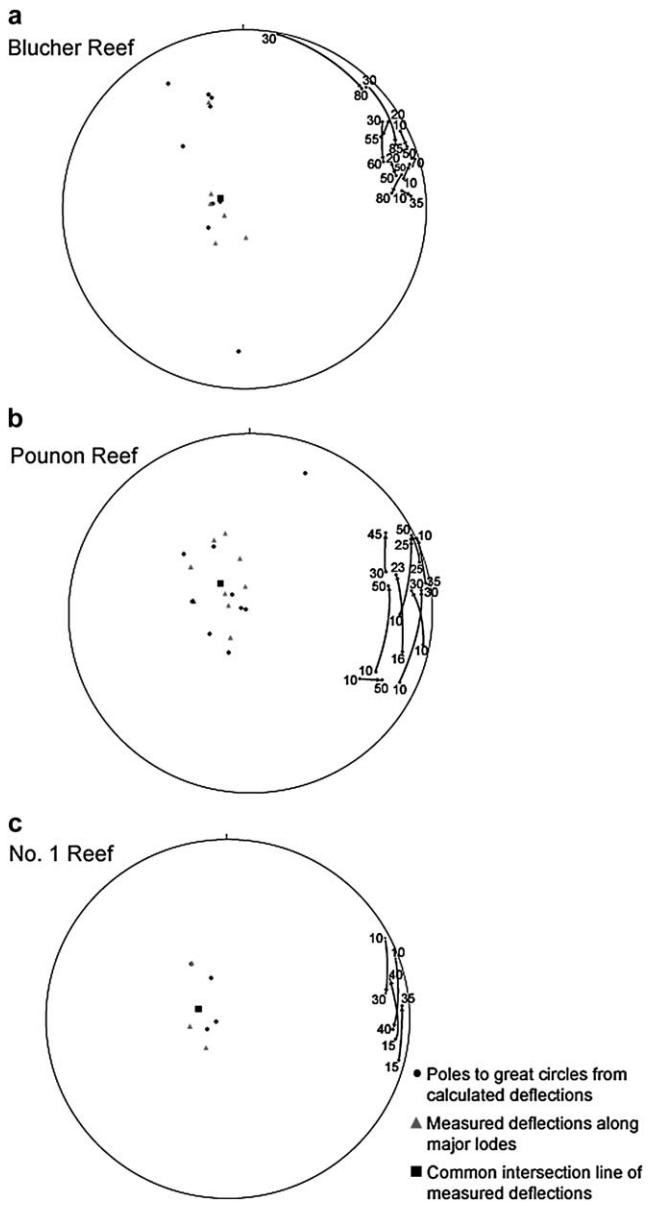

Fig. 6. Pairs of poles from vein deflections, linked by partial great circles, shown in lower hemisphere equal area nets. Arrow heads point towards the thicker segment (Nortje, 2004). Triangles show measured deflections along major veins.

(Figs. 4 and 7) indicating a large shear component during the formation of these fractures.

The orientation of the slip vectors is almost parallel to the deflection lines (especially in the Pounon Reef). This may be a situation analogous to that in linked normal faults (e.g. Acocella et al., 2000) where the slip vector is also sub-parallel to the intersection line between the segments.

5.2. Other displacement or slip data

Although the Broken Hills veins are geometrically simple, they contain evidence of complex adjustments during and after vein formation (Nortje, 2004). Although most striations coeval with vein formation show dip-slip movement compatible with the slip vector determined from the vein deflections, there are some that indicate local strike slip movement. A phase of strike-slip faulting and some of the brecciation postdates the formation of the main lodes.

6. Vein thickness distributions

Minor quartz vein thickness distributions are fractal with $D = 1.2 \pm 0.09$ ($n = 127$) (Fig. 9a). Such fractal vein thickness distributions are characteristic of non-stratabound veins, in agreement with the inference that the mechanical anisotropy of the host rock does not influence the formation of brittle structures (Gillespie et al., 1999; Nortje, 2004). This D-value is towards the upper range of values recorded from non-stratabound extensional veins in the literature (e.g. Gillespie et al., 1999). Breccia veins also have a fractal vein thickness distribution. However, their D-value is 0.9 ± 0.08 ($n = 98$), significantly lower than for the quartz vein thickness distribution (Fig. 9b).

7. Evolution of the Broken Hills mineralising system

Mesoscopic veins form simple patterns and are similar in the three major lode systems at Broken Hills. Their vein deflection axes plunge steeply down the overall steep westward dip of the veins. Horizontal separation vectors as defined in Figs. 4 and 7 trend NW-SE for dextral deflections and NE-SW for sinistral deflections (Fig. 8).

Because of the coherence of these geometric data, we have applied a slip model linking opening on all of the deflected veins (Fig. 4). More complex geometry and 3-D strain conditions (Irwin, 2004) would apply during opening of triple and quadruple vein junctions. In our example, the intersection of movement planes defined by the horizontal separation vector and the corresponding deflection line yield consistent steeply plunging opening vectors (Figs. 7 and 8).

This result has an important consequence for the formation of the Broken Hills vein system because of the non-orthogonal opening vector, these veins are not pure extension veins but have experienced considerable shearing parallel to the vein walls during opening (Brown and Bruhn, 1996).

7.1. Evolution of Broken Hills epithermal Au-Ag deposit

The vein geometries and thickness distributions suggest a possible model for the formation of Broken Hills epithermal Au-Ag deposit, given that mineralization formed within the upper 200 m of a fossil geothermal system as indicated by the presence of sinters (Section 2.1). It is likely that hydrostatic fluid pressures along with low differential and effective stresses were present at the time of mineralization.

Kinematic evidence along the main lodes (Fig. 1a) implies a dip-slip sense of movement. Steep westerly plunging vein deflections also imply that a large component of normal dip-slip movement occurred along the major structures as shown in Fig. 4. Initially many isolated extension veins (quartz veins)

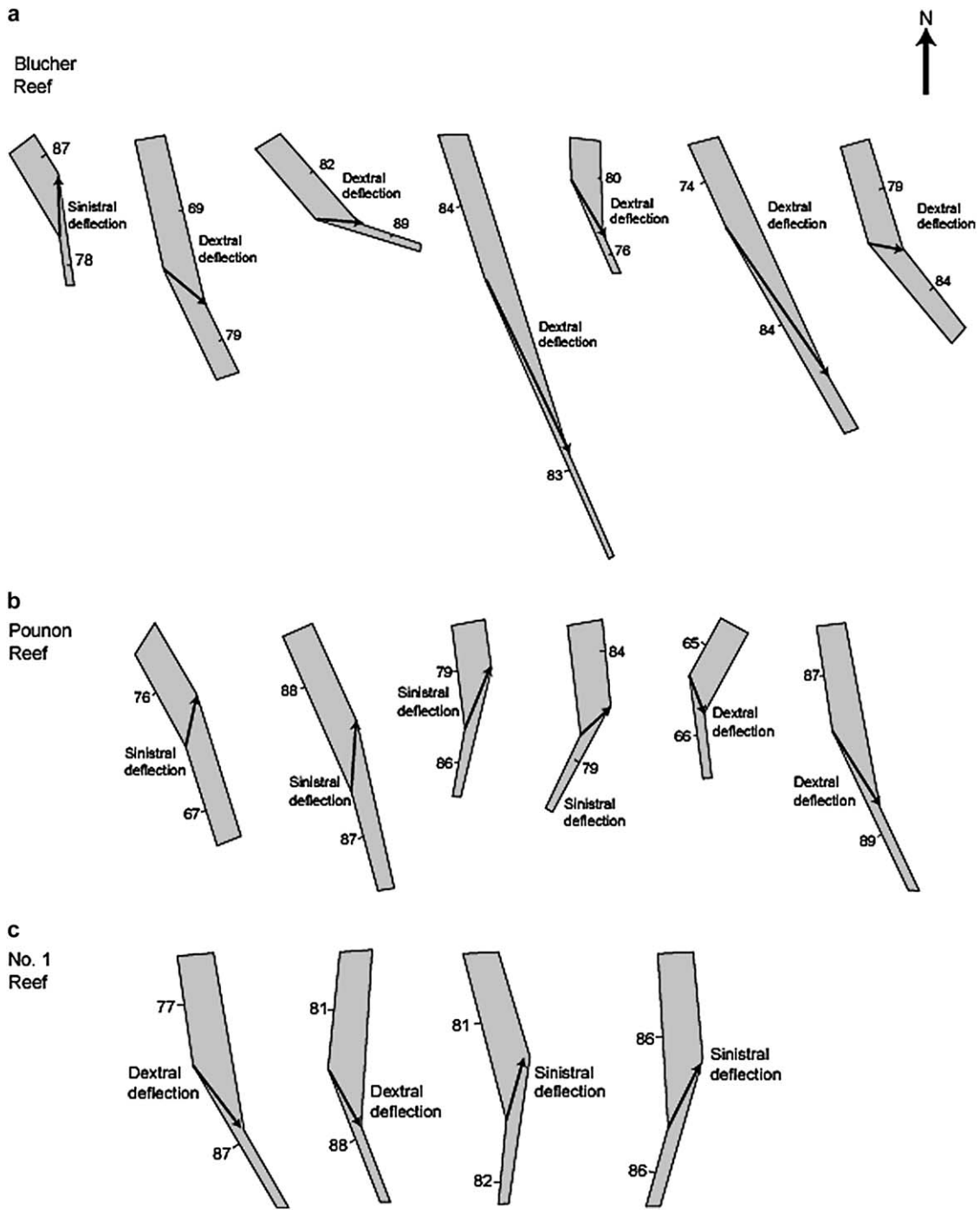

Fig. 7. Examples of thickness variations and separation vectors in the horizontal plane from the three main reefs (Nortje, 2004). Sense of deflection is as defined in Fig. 4a. Thicknesses are normalised to that of the thicker segment.

develop (Fig. 10a) with many small relative to thick veins, which obey a power law distribution where $D = 1.2 \pm 0.09$ ($n = 127$) (Fig. 9), which is not atypical for non-stratabound vein arrays (Gillespie et al., 1999). During this time veins were unconnected. Extensional shears developed by linkage of the extension veins, and obey a power law distribution, with $D = 0.9 \pm 0.08$ (Fig. 10b) resulting in a system of linked extension veins and extensional shears as attested by the dip slip movement on the main lode (Figs. 2 and 10b). The extensional shears have a lower fractal dimension than the extension veins because the fault linkage required to form them restricted the variations in thickness, resulting in a lower fractal dimension (Fig. 10c).

A possible implication of the model is that permeability may be created in a horizontal direction by linkage of extension veins and extensional shears, and in a vertical direction by the bends/jogs in the extensional shears. This overcomes some of the difficulties with the fracture mesh concept where

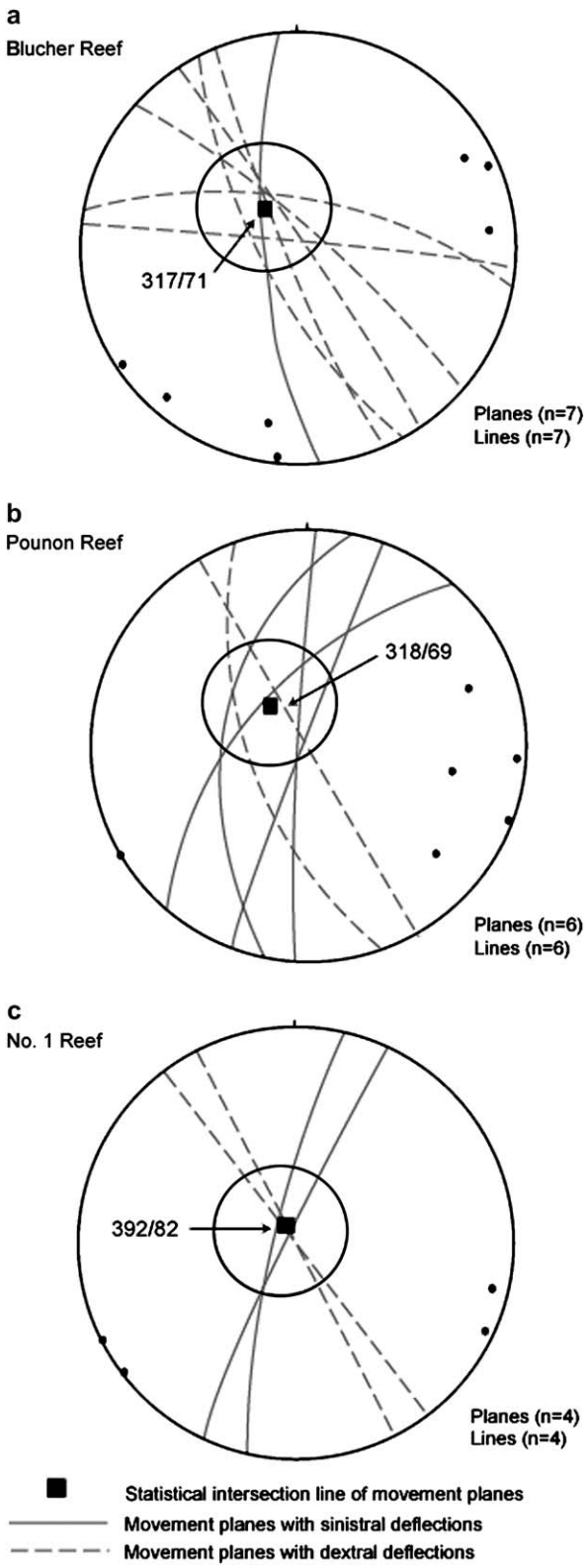

Fig. 8. Determination of opening vectors (indicated by bearing and plunge, e.g. 317/71) from the intersection of movement planes for the three main reefs. 99% confidence interval calculated after Allmendinger (2002).

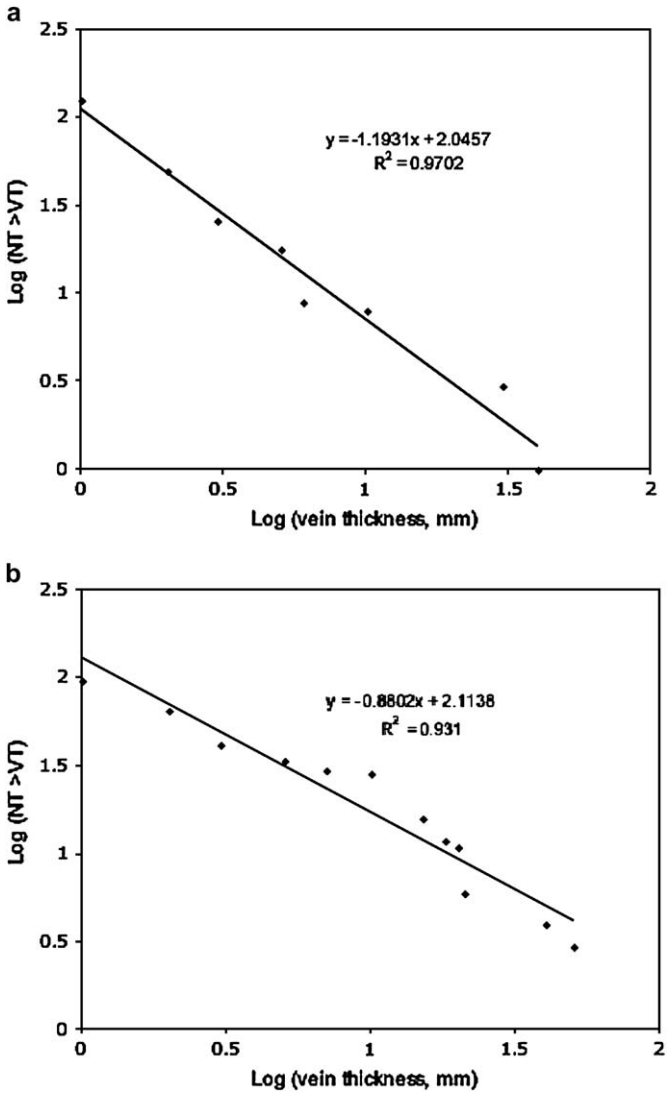

Fig. 9. (a) Quartz vein thickness distribution on a log-log plot. The equation gives the regression line, the slope being the fractal dimension; and (b) breccia vein thickness distribution on a log-log plot. The equation gives the regression line, the slope being the fractal dimension (Nortje et al., 2005).

the greatest permeability is in a horizontal direction (in normal fault systems) whereas vertical fluid flow is required for the formation of an epithermal ore deposit.

8. Conclusions

A method of analysing the opening kinematics of veins has been developed and combined with vein thickness distributions to understand the evolution of the vein network at Broken hill epithermal gold deposit in the Coromandel peninsula, New Zealand. The method allows the construction of vein opening vectors from a set of non-planar veins.

Vein deflections at Broken Hills imply that extensive normal faulting has occurred within the deposit in a system of extensional veins, which initially grew as independent structures in a non-stratabound array, and were then linked by segmented extensional shears. Vein thickness distributions are

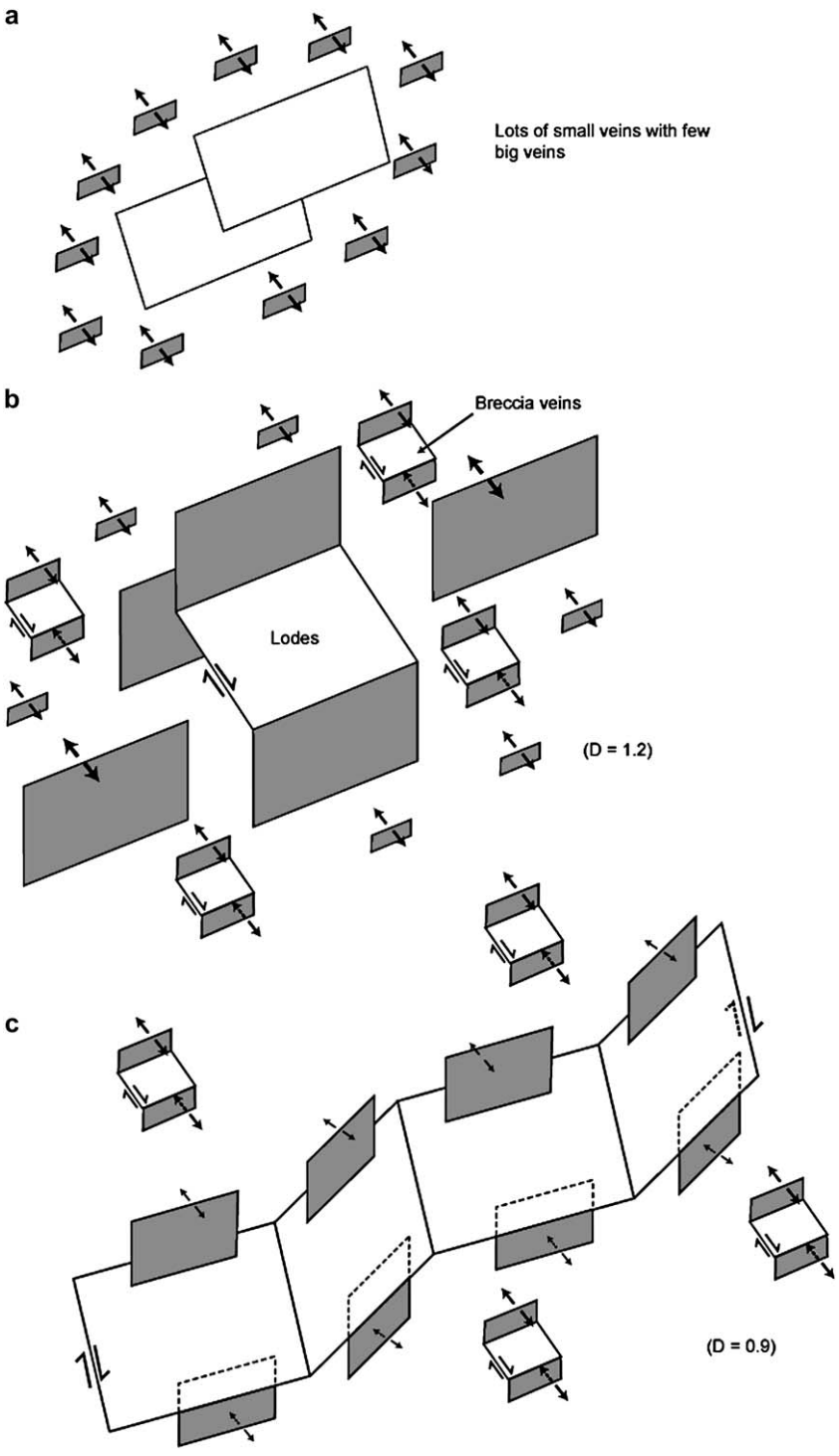

Fig. 10. A possible mechanism for vein formation at Broken Hills: (a) isolated extensional veins, leading to a population with many thin relative to thick veins; (b) the breccia veins may have originated as extensional shears in a system of linked normal faults; and (c) linked extension veins and extensional shears.

power law with $D = 1.2 \pm 0.09$ for extension veins and $D = 0.9 \pm 0.08$ for extensional shears. Extension veins evolved with many thin relative to thick veins followed by extensive fault linkage to form the extensional shears. Broken Hills also provides a clear example of non-plane, 3D − strain in an epithermal deposit. Intensive application of the slip determination method outlined in the present paper, combined with statistical investigation of vein parameter distribution can provide vital information on the mineralisation pathways in epithermal deposits, even for vein systems more complex than that of Broken Hills.

Acknowledgements

Financial support was provided by the New Zealand Foundation for Research, Science and Technology (FRST). G.S.N

thanks Professor Nick Oliver for thoughtful and encouraging discussions. We thank Ken McCaffrey and Dave Craw for thoughtful and constructive reviews that greatly improved the manuscript.

References

Acocella, V., Gudmundsson, A., Funiciello, R., 2000. Interaction and linkage of extension fractures and normal faults: examples from the rift zone of Iceland. Journal of Structural Geology 22, 1233–1246.

Ballance, P.F., 1976. Evolution of the upper Cenozoic magmatic arc and plate boundary in northern New Zealand. Earth and Planetary Science Letters 28, 356–370.

Bell, J.M., Fraser, C., 1912. The Geology of the Waihi-Tairua Subdivision, Hauraki Division. Government Printer, Wellington.

Brathwaite, R.L., Christie, A.B. 1986. A comparison of epithermal mineralisation in the Hauraki Goldfield and Geothermal Systems of the Taupo Volcanic Zone. In: International Volcanological Congress: Proceedings of Symposium 5: Volcanism, Hydrothermal Systems and Related Mineralisation.

Brathwaite, R.L., Christie, A.B., Skinner, D.N.B. 1989. The Hauraki Goldfield – regional setting, mineralisation and recent exploration. In: Kear, D. (Ed.), Mineral Deposits of New Zealand – Monograph, 13, pp. 45–56.

Brown, S.R., Bruhn, R.L., 1996. Formation of voids and veins during faulting. Journal of Structural Geology 18 (5), 657–671.

Christie, A.B., Brathwaite, R.L. 1986. Epithermal gold-silver and porphyry copper deposits of the Hauraki goldfield – a review. In: Henley, R.W., Hedenquist, J.W., Roberts, P.J. (Eds.), Guide to the Active Epithermal (Geothermal) Systems and Precious Metal Deposits of New Zealand. Monograph Series on Mineral Deposits No. 26, pp. 129–145.

Cox, S.F., 1987. Antitaxial crack-seal vein microstructures and their relationship to displacement paths. Journal of Structural Geology 9, 779–787.

Cox, S.F., Wall, V.J., Etheridge, M.A., Potter, T.F., 1991. Deformational and metamorphic processes in the formation of mesothermal vein-hosted gold deposits – examples from the Lachlan Fold Belt in central Victoria, Australia. Ore Geology Reviews 6, 391–423.

Cox, S.F., Knackstedt, M.A., Brawn, J., 2001. Principles of structural control on permeability and fluid flow in hydrothermal systems. In: Richards, J.P., Tosdal, R.M. (Eds.), Structural Controls on Ore Genesis. Reviews in Economic Geology 14. Society of Economic Geologists, Littleton, CO, pp. 1–22.

Gadsby, M.R., Spörli, K.B., Clarke, D.S., 1989. Structural elements in epithermal gold deposits of the Coromandel: a review. In: Proceedings of the 11th New Zealand Geothermal Workshop, pp. 149–154.

Gillespie, P.A., Johnston, J.D., Lorgia, M.A., McCaffrey, K.J.W., Walsh, J.J., Watterson, J., 1999. Influence on layering on vein systematics in line samples. In: McCaffrey, K.J.W., Lonergan, L., Wilkinson, J.J. (Eds.), Fractures, Fluid Flow and Mineralization 155. Geological Society of London, London, pp. 35–56.

Irwin, M.R., 2004. The Structure of Epithermal Deposits of the Coromandel Peninsula: Dynamic Processes and Three-Dimensional Strain. Unpublished PhD thesis, University of Auckland, New Zealand.

Johnston, J.D., McCaffrey, K.J.W., 1996. Fractal geometries of vein systems and the variation of scaling relationships with mechanism. Journal of Structural Geology 18 (2/3), 349–358.

Koehn, D., Passchier, C.W., 2000. Shear sense indicators in striped bedding-veins. Journal of Structural Geology 22 (8), 1141–1151.

Koehn, D., Hilgers, C., Bons, P.D., Passchier, C.W., 2000. Numerical simulation of fibre growth in antitaxial strain fringes. Journal of Structural Geology 22 (9), 1311–1324.

Lorgia, M.A., 1999. Scaling systematics of vein size: an example from the Guanajuato mining district (Central Mexico). In: McCaffrey, K.J.W., Lonegran, L., Wilkinson, J.J. (Eds.), Fractures, Fluid Flow and Mineralisation. Geological Society Special Publication 155. Geological Society, London, pp. 57–67.

Marrett, R., 1996. Aggregate properties of fracture populations. Journal of Structural Geology 18 (3), 169–178.

McCaffrey, K.J.W., Johnston, J.D., 1996. Fractal analysis of a mineralised vein deposit: Curraghinalt gold deposit County Tyrone. Mineralium Deposita 31, 52–58.

Nortje, G.S. 2004. Structural Aspects of Mineralisation at the Broken Hills epithermal Au-Ag Deposit, Coromandel Peninsula, New Zealand. Unpublished MSc thesis, University of Auckland, New Zealand.

Nortje, G.S., Blenkinsop, T., Rowland, J.V., 2005. Evidence from fractal thickness distributions for the evolution of vein systems in a rhyolite-hosted epithermal deposit. In: Hancock, H., Fisher, L., Baker, T., Bell, T., Blenkinsop, T., Chapman, L., Cleverley, J., Collins, B., Duckworth, R., Evins, P., Ford, A., Oliver, N.H.S., Rubenach, M., Williams, P. (Eds.), Structure, Tectonics, Ore Mineralisation Processes. Economic Geology Research Unit, Townsville, p. 199.

Ramsay, J.G., 1980. The crack-seal mechanism of rock deformation. Nature 284, 135–139.

Ramsay, J.G., Huber, M.I., 1983. The Techniques of Modern Structural Geology. In: Folds and Fractures, Vol. 2. Academic Press, London.

Roberts, S., Sanderson, D.J., Gumiel, P., 1999. Fractal analysis and percolation properties of veins. In: McCaffrey, K.J.W., Lonegran, L., Wilkinson, J.J. (Eds.), Fractures, Fluid Flow and Mineralisation. Geological Society Special Publication 155. Geological Society, London, pp. 7–16.

Rowland, J.V., Sibson, R.H., 2004. Structural controls on hydrothermal fluid flow in a segmented rift system, Taupo Volcanic Zone. Geofluids 4, 259–283.

Sanderson, D.J., Roberts, S., Gumiel, P., 1994. A fractal relationship between vein thickness and gold grade in drill core from La Codosera, Spain. Economic Geology 89, 168–173.

Sibson, R.H., 1987. Earthquake rupturing as a mineralizing agent in hydrothermal systems. Geology 15, 701–704.

Sibson, R.H., 1996. Structural permeability of fluid-driven fault-fracture meshes. Journal of Structural Geology 18 (8), 1031–1042.

Sibson, R.H., 2001. Seismogenic framework for hydrothermal transport and ore deposition. In: Richards, J.P., Tosdal, R.M. (Eds.), Structural Controls on Ore Genesis. Reviews in Economic Geology 14. Society of Economic Geologists, Littleton, CO, pp. 25–47.

Skinner, D.N.B. 1986. Neogene volcanism in the Hauraki volcanic region. In: Smith, I.E.M. (Ed.), Late Cenozoic Volcanism in New Zealand. Royal Society of New Zealand Bulletin 23, pp. 20–47.

Smith, J.V., 2005. Textures recording transient porosity in synkinematic quartz veins, South Coast, New South Wales, Australia. Journal of Structural Geology 27 (2), 357–370.

Stowell, J.F.W., Watson, A.P., Hudson, N.F.C., 1999. Geometry and population systematics of a quartz vein set, Holy Island, Anglesey, North Wales. In: McCaffrey, K.J.W., Lonegran, L., Wilkinson, J.J. (Eds.), Fractures, Fluid Flow and Mineralisation. Geological Society of London, London, pp. 17–33. Special Publication 155.

Urai, J.L., Williams, P.F., van Roermund, H.L.M., 1991. Kinematics of crystal growth in syntectonic fibrous veins. Journal of Structural Geology 13 (7), 823–836.

Wilkinson, J.J., Johnston, J.D., 1996. Pressure fluctuations, phase separation, and gold precipitation during seismic fracture propagation. Geology 24 (5), 395–398.